Int J Thermophys (2007) 28:1800–1811
DOI 10.1007/s10765-007-0269-9

A Noise Thermometer for Practical Thermometry at Low Temperatures

Jost Engert · Jörn Beyer · Dietmar Drung · Alexander Kirste · Margret Peters

Published online: 3 October 2007

Abstract The application of a magnetic-field-fluctuation thermometer (MFFT) is described for practical thermometry in the low-temperature range. The MFFT inductively measures the magnetic noise generated by Johnson noise currents in a metallic temperature sensor. The temperature of the sensor is deduced from its thermal magnetic noise spectrum by applying the Nyquist theorem, making the thermometer in principle linear over a wide range of temperatures. In this setup, a niobium-based dc SQUID gradiometer detects the magnetic field fluctuations. The gradiometer design optimizes the inductive coupling to the metallic temperature sensor, yet equally ensures sufficient insensitivity to external magnetic interference. In order to obtain a highly sensitive and fast thermometer, the SQUID chip is placed directly onto the surface of the temperature sensor. The compact setup of the gradiometer/temperature sensor unit ensures good conditions for thermal equilibration of the sensor with the temperature to be measured, a factor that becomes increasingly important in the temperature range below 1 K. The first direct comparison measurements of the MFFT with a high-accuracy realization of the Provisional Low Temperature Scale of 2000 (PLTS-2000) are presented. Special emphasis is given to the investigation of the linearity, speed, and accuracy of the MFFT.

Keywords Noise thermometry · PLTS-2000 · SQUID magnetometry

1 Introduction

In the temperature range below 1 K, currently two international temperature scales exist, the International Temperature Scale of 1990 (ITS-90) [1] and the Provisional

J. Engert (✉) · J. Beyer · D. Drung · A. Kirste · M. Peters
Physikalisch-Technische Bundesanstalt, Abbestrasse 2-12, Berlin 10587, Germany
e-mail: jost.engert@ptb.de

Low Temperature Scale of 2000 (PLTS-2000) [2,3], which can be used for traceable temperature measurements. The ITS-90 extends from higher temperatures down to 0.65 K whereas the PLTS-2000 ranges from 0.9 mK to 1 K. In the range of overlap, the ITS-90 deviates systematically from thermodynamic temperature. Therefore, the Consultative Committee for Thermometry of the BIPM [4] recommends that the PLTS-2000 is preferred, on the grounds of both better thermodynamic accuracy and the potential for lower uncertainty of realization. Recently, a new ^{3}He vapor-pressure based temperature scale, the PTB-2006 [5], has been established for the temperature range from 0.65 to 3.2 K. The PTB-2006 removes the thermodynamic inconsistency of the ITS-90 below 1.2 K and is consistent with the PLTS-2000.

However, for practical thermometry below 1 K, the realization of the above mentioned temperature scales is expensive and time-consuming. The same applies to primary thermometry techniques such as nuclear orientation and noise thermometry. Secondary thermometers provide an alternative, but need to be calibrated.

Here, we describe a new variant of a noise thermometer, the magnetic-field-fluctuation thermometer (MFFT) [6,7], for use as a secondary or semi-primary thermometer. For the MFFT presented here, standard and commercially available dc SQUID techniques and electronics are employed. The MFFT has a linear characteristic, is easy to use, fast, robust, and of small dimensions. To avoid the elaborate determination of all parameters of the measurement chain, as would be necessary for its application as a primary thermometer, the MFFT was calibrated at a single reference temperature. Then, with the measurement parameters determined, the MFFT was investigated in the temperature range from about 0.7 K down to 0.007 K.

2 The MFFT Thermometer

2.1 Principle of Operation

Noise thermometry is one of the most developed methods of primary thermometry below 1 K [8]. It is based upon the measurement of the noise generated by the thermal agitation of electric charge carriers in a conductor, which are in thermal equilibrium. Hence, the conductor is the actual temperature sensor in all noise thermometer types. The basic working principle of the MFFT is the *inductive* detection of magnetic field fluctuations or thermal magnetic noise in the vicinity of the conductor. The Brownian motion of the charge carriers inside the conductor can be considered to form a multitude of closed-loop noise current modes [9,10] causing the magnetic-field fluctuations that, in turn, can be related to temperature via Nyquist's relation for the noise current in a conductor. With the recent development of SQUID technology, it became possible to reliably measure such tiny field fluctuations.

The advantage of the MFFT is that neither electrical nor thermal contact is required between the measurement system and the temperature sensor whose temperature is to be measured. This is of crucial importance in the low-temperature region, especially below 1 K, where any heat input to the temperature sensor can increase its temperature because of the rapidly increasing thermal resistances. Furthermore, the metallic temperature sensor can be adapted to provide good thermal contact to the measuring

object as well as occupy a volume of sufficient size to avoid hot-electron effects [11] (see Sect. 4.2.). On the other hand, the absolute value of the resistive impedance of the MFFT is rather difficult to determine with the uncertainty required for primary thermometry.

In order to build a MFFT for the low temperature range, two components are needed: a temperature sensor made of a material with an electrical conductivity highly constant in that temperature range, and a magnetometer sensitive enough to detect the thermal magnetic noise. The natural magnetic field sensor to be used with a low temperature MFFT is a magnetometer based on the dc SQUID [12]. A bare dc SQUID is a highly sensitive detector of magnetic flux changes. A SQUID magnetometer comprises a SQUID and an antenna for magnetic flux, and it detects integral magnetic field changes over the area of its flux antenna. Therefore, the thermal magnetic field noise is sensed by the SQUID as thermal magnetic flux noise (TMFN). For a given configuration of conductor geometry and SQUID magnetometer, the TMFN detected originates predominantly from parts of the conductor volume closest to the flux antenna.

In order to extract the temperature information from the TMFN, we choose to analyze the noise frequency spectrum, although a time-domain analysis would be equally applicable. From Nyquist's noise theorem, it follows that the power spectral density (PSD) of the noise is proportional to thermodynamic temperature, T. The PSD of the TMFN, S_Φ, detected by the SQUID magnetometer as a function of frequency f is of "low-pass-like" form and can be described by the following empirical equation:

$$S_\Phi(f, T) = S_0(T) \Big/ \left(1 + \left(\frac{2}{\pi}\frac{f}{f_c}\right)^{2p_1}\right)^{p_2} \tag{1}$$

Here, $S_0(T)$ is the zero-frequency value of $S_\Phi(f, T)$ and f_c is a characteristic frequency of the fall-off of the detected noise. For a fixed geometry of the conductor and the SQUID magnetometer and a constant conductivity σ, the value of $S_0(T)$ is directly proportional to the sensor temperature. Moreover, if σ does not vary with T, the characteristic frequency f_c as well as the exponents p_1 and p_2 are also constant, with p_1 and p_2 approximately equal to 1. Then, a given MFFT setup exhibits a characteristic frequency dependence of S_Φ which is independent of temperature. It is, therefore, possible to operate the MFFT as a semi-primary thermometer. In this case, the device characteristic parameters $S_0(T_{\mathrm{ref}})$, f_c, p_1, and p_2 of the PSD are determined at one known reference temperature T_{ref}, and the temperature T to be measured is obtained from the simple relation:

$$T = T_{\mathrm{ref}} \frac{S_0(T)}{S_0(T_{\mathrm{ref}})} \tag{2}$$

For the purpose of choosing a suitable shape of the metallic temperature sensor, the magnetic flux antenna can be considered as a system with one degree of freedom, which is the magnetic energy stored in the inductance L of the flux antenna. The total thermal energy of this system equals $k_B T/2$, and is unchanged by the presence of the temperature sensor. The effect of the electrically-conducting temperature sensor is to influence the frequency distribution of the flux antenna's thermal energy in the frequency domain [13]. Therefore, for a fixed flux antenna and a conductor of given

conductivity, the geometric configuration can be optimized in order to "tailor" the TMFN spectrum to provide a sufficiently high zero-frequency value $S_0(T)$ compared to the intrinsic flux noise of the SQUID as well as to exhibit a high characteristic frequency f_c. The characteristic frequency is a measure of the speed of the MFFT, i.e., the time needed for a temperature measurement with a given accuracy. The TMFN at frequencies below f_c arises from noise current modes exhibiting smaller spatial frequencies than the modes predominantly contributing to the noise spectrum above f_c. Therefore, at $f > f_c$ the SQUID magnetometer senses the TMFN originating from ever-smaller regions of the conductor, a potentially adverse measurement condition if thermal gradients are present. Also, with the thermal magnetic noise falling off with frequency, typically so does the ratio of the TMFN to the SQUID noise. Therefore, the MFFT noise temperature T_N, defined as the temperature at which the TMFN equals the SQUID noise, increases for $f > f_c$.

2.2 Design and Realization

Recently, we have demonstrated the functionality of an integrated MFFT operated in the temperature range of 4.5–0.3 K [7]. We continue to develop MFFT implementations in order to obtain a more compact thermometer which, in addition, is highly robust against external magnetic fields. Furthermore, we aim at improving the speed of the thermometer, i.e., increasing f_c and reducing T_N over an extended frequency range. In Fig. 1, the setup used for MFFT measurements in the temperature range below 1 K is depicted. It consists of a bottom and a top part made from high purity Cu (99.999%, <1 ppm Fe), a $3 \times 3\,\mathrm{mm}^2$ SQUID chip directly placed onto the bottom part, and a printed circuit board used for the electrical connection to the SQUID electronics. Wiring is fed through a bore in the bottom Cu part. The bottom and top parts are screwed together, both forming the temperature sensor and encapsulating the SQUID chip. The latter provides an eddy-current shield against external magnetic interference.

The SQUID chip is placed at the center of the bottom Cu part which has been thinned to about 250 μm. Simulations and experiments suggested reducing the Cu thickness

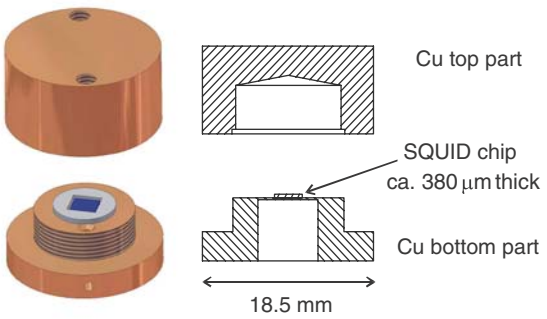

Fig. 1 Setup for the MFFT. For details, refer to the text

beneath the SQUID chip in the manner shown, in order to optimize the spectral shape of the TMFN sensed by the SQUID.

The thermal magnetic fields threading the flux antenna are, by their nature, characterized by uncorrelated spatial and temporal gradients. SQUID sensors with a gradiometric flux antenna are, therefore, well-suited to MFFT purposes. In this way, the MFFT setup becomes highly insensitive to homogeneous magnetic fields not originating from the TMFN of the temperature sensor. The integrated MFFT setup reported here makes use of a thin-film multiloop SQUID magnetometer with an on-chip gradiometric flux antenna specifically designed for MFFT use. The flux antenna encloses a total area of ca. 6 mm^2. However, the gradiometer configuration makes the SQUID virtually insensitive to homogeneous magnetic fields. In the SQUID design for the MFFT setup used here, the feedback coil was designed to present a sufficiently large mutual inductance to the SQUID, but at the same time minimal inductive coupling to the temperature sensor. In this way, the coupling of the intrinsic noise of the SQUID and of the read-out electronics noise to the temperature sensor is minimized. Further details of the layout will be published elsewhere.

3 Experimental

3.1 Realization of the PLTS-2000

A detailed description of the experimental setup for the realization of the PLTS-2000 at PTB is given in [14]. The calibration of the melting-pressure sensor was made at one of the pressure fixed points of the PLTS-2000, the minimum, and, in addition, at two calibrated superconductive reference point samples. This procedure is practicable for cryostats which do not reach temperatures below 0.005 K. In this case, the low-temperature natural features of the melting curve are not available as fixed points of pressure and temperature [2]. Nevertheless, the uncertainty is not much larger than for the realization of the PLTS-2000 using the low-temperature features. During the experiments, the calibration of the melting-pressure sensor was checked several times. In addition, the temperature values according to the PLTS-2000, T_{2000}, were permanently compared with the temperature indication of a rhodium–iron resistance thermometer carrying a copy of the PLTS-2000 as well as with a very stable carbon resistance thermometer. In the temperature range of interest here, the expanded uncertainty ($k = 2$) for the T_{2000} values is of the order of 0.06 mK temperature equivalent, except in the region near the pressure minimum. The uncertainty budget for the PLTS-2000 realization, which lists in detail the relevant uncertainty components, can be found in [5] and the references therein.

3.2 SQUID Electronics and Data Acquisition System

Figure 2 depicts a schematic diagram of the MFFT measurement. The SQUID is operated in a flux locked loop (FLL) [15]. Time records of the analog FLL output signal were anti-alias-filtered (2nd-order Bessel-type low-pass filter, $f_{3dB} = 10$ kHz), digitized, and Fourier-transformed using a commercial fast-Fourier-transform (FFT)-analyzer

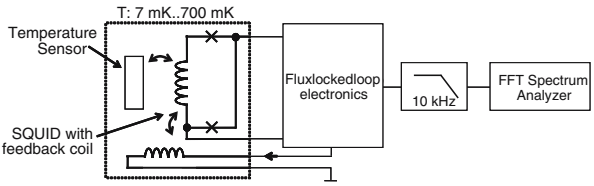

Fig. 2 Schematic diagram of the MFFT including the metallic noise temperature sensor, the SQUID, and the measurement electronics

to obtain the TMFN spectra. The individual time records of 1 and 2 s length were transformed into spectra with line numbers $N_{\text{lines}} = 800$ and resolution bandwidths of 1 and 0.5 Hz, respectively. No overlap of the time records was used and averaging of the spectra was performed in the frequency domain.

4 Operation of the MFFT in the Temperature Range of the PLTS-2000

4.1 Measurements

To investigate the MFFT as a semi-primary thermometer, different measurement series were carried out. Firstly, TMFN spectra were taken in the frequency ranges from 10 to 400 Hz and from 10 to 800 Hz at a stabilized reference temperature T_{ref} of about 0.676 K. To reduce as much as possible the statistical uncertainty, each spectrum was averaged 22,000 times. These spectra served as calibration spectra for further analysis (see Sect. 4.2). The corresponding data are displayed in Fig. 3 by the trace labeled 'a' and in Fig. 4 by the solid red line. Then, spectra were taken at stabilized temperature plateaux with successively lower temperature levels from 0.6 K down to the mK region. For the 10–800 Hz range (Fig. 3), the spectra were averaged 22,000 times, whereas for the 10–400 Hz range (Fig. 4), only 100 averages were taken. The measuring times t_{meas} amounted to 22,000 and 200 s, respectively.

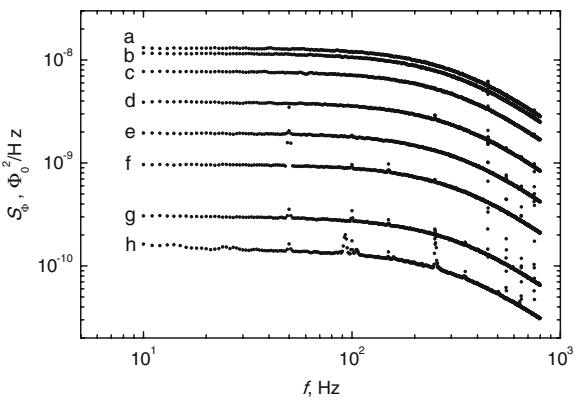

Fig. 3 Spectra of the TMFN in the frequency range from 10 to 800 Hz averaged 22,000 times. Traces labeled from 'a' to 'h' correspond to temperatures T_{2000} of 0.676, 0.597, 0.399, 0.200, 0.100, 0.050, 0.015, and 0.007 K, respectively

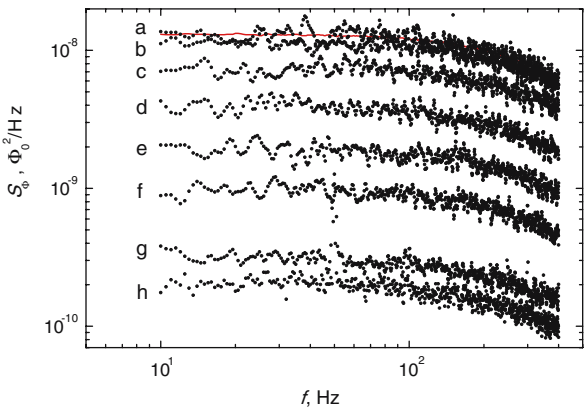

Fig. 4 Spectra of the TMFN in the frequency range from 10 to 400 Hz averaged 100 times. Traces labeled from 'a' to 'h' correspond to temperatures T_{2000} of 0.676, 0.597, 0.399, 0.200, 0.100, 0.050, 0.015, and 0.010 K, respectively. Solid red line depicts the 22,000 times averaged reference spectrum at 0.676 K

It can be clearly seen in Figs. 3 and 4 that the frequency dependence of all noise spectra exhibits the expected low-pass form and the noise level decreases with decreasing temperature. In the low frequency range, the spectral noise densities are nearly constant. Only in the spectrum for the long averaging time at 0.007 K (trace 'h' in Fig. 3) is a slight upturn of the noise level at low frequencies visible. This is probably caused by intrinsic low-frequency noise of the SQUID that only becomes relevant when the level of the TMFN is substantially reduced at the lowest temperatures.

To examine the stochastic behavior of the MFFT, noise spectra were measured as a function of the number of averages N_{avg}. In one series at 0.015 K, N_{avg} ranged from 1 to 22,000 for the frequency range from 10 to 400 Hz and, in a second series at 0.05 K, N_{avg} ranged from 3,000 to 22,000 for the frequency range from 10 to 800 Hz.

In addition, at 0.015 and 0.05 K, the dependence of the spectra on the electrical SQUID bias power dissipated in the MFFT module was investigated. For this purpose, the working point of the SQUID was changed by varying the bias current and bias voltage [15]. The electrical power dissipation was estimated from the product of the bias current applied to the SQUID and the SQUID bias voltage. The change in the noise level of the SQUID itself caused by the change in the SQUID bias parameters was taken into account. The corresponding spectra were averaged over 7,200 s in the frequency range from 10 to 800 Hz.

4.2 Results

For the MFFT used, the geometrical parameters are fixed and the electrical conductivity of the metallic noise sensor is assumed to be independent of temperature. The zero frequency values $S_0(T)$ were extracted from fits to the TMFN spectra. Then, the temperature indication T_{MFFT} of the MFFT was obtained using Eq. 2.

To improve the data processing, the spikes at the mains frequency and its higher harmonics were removed from the measured noise spectra. This was necessary because the results of the noise spectra fits appeared to be influenced by the amplitude of those spikes, even when the absolute power contained in these narrow frequency bands

is negligible. The spikes were present in our first MFFT setup. Our revised MFFT setup used improved wiring inside the cryostat, eliminating the external magnetic interference from the mains in subsequent experiments. From all spectra, a constant noise floor was subtracted in order to take into account the noise of the SQUID itself that was always present in the measurements. An estimate of $1 \times 10^{-12}\Phi_0^2/\mathrm{Hz}$ was applied for the SQUID noise, including the room temperature amplifier noise. Next, from a least-squares fit of the calibration spectra taken at the reference temperature $T_{\mathrm{ref}} = T_{2000} = 0.676\,\mathrm{K}$, the constants $S_0(T_{\mathrm{ref}})$, f_c, p_1, and p_2 were determined. Then, for every stabilized temperature, the averaged noise spectra were fitted keeping f_c, p_1, and p_2 fixed and T_{MFFT} was derived from $S_0(T)$ using Eq. 2. The Type A uncertainty component for T_{MFFT} was estimated from the standard errors of the fit parameters.

Figure 5 shows the dependence of the relative Type A uncertainty u_r for T_{MFFT} on the number of averages N_{avg} of the spectra taken at 0.015 K in the frequency range from 10 to 400 Hz. As expected for a statistical process, u_r follows $1/\sqrt{N_{\mathrm{avg}}}$. The data can be described by $u_r = 1.0428/\sqrt{N_{\mathrm{avg}}N_{\mathrm{lines}}}$. For more than 20 averages, corresponding to t_{meas} longer than 40 s, u_r is already smaller than 1%. The same behavior is found for the dependence of the Type A uncertainty component on N_{avg} for the noise measurements carried out at 0.05 K.

In Fig. 6, the deviation of T_{MFFT} from T_{2000} is depicted for the corresponding measurements shown in Fig. 5. Here, the expanded uncertainties ($k = 2$) are included. The Type B uncertainty components are estimated from the uncertainties caused by the measurement system and from a contribution taking into account a systematic deviation of T_{MFFT} from T_{2000}. With increasing N_{avg}, the temperatures T_{MFFT} tend to a constant value which is, nevertheless, slightly higher than T_{2000}. This may be caused by additional noise contributions other than those described by Eq. 1 or by overheating of the noise sensor (see below). A more detailed investigation of possible sources of uncertainty contributions is in progress.

The comparison of the MFFT temperatures deduced from the noise spectra for the frequency range from 10 to 800 Hz averaged over 22,000 s with the realization of the PLTS-2000 in temperature for nearly two decades is presented in Fig. 7. The T_{MFFT} values closely follow T_{2000} down to 0.007 K. From 0.6 to 0.05 K, the relative deviation

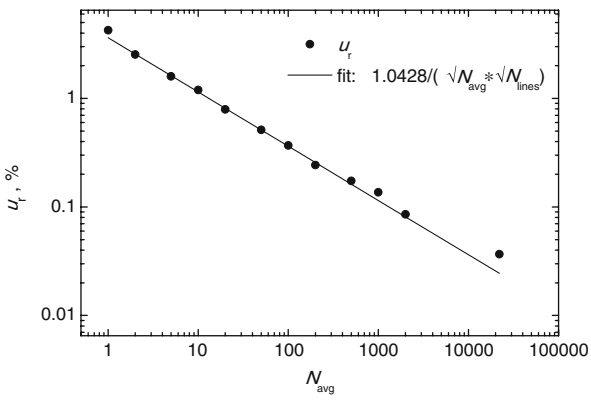

Fig. 5 Relative Type A uncertainty component u_r of the TMFN measurements versus the number of averages N_{avg} at $T_{2000} = 0.015\,\mathrm{K}$. Frequency range for the TMFN measurements is from 10 to 400 Hz

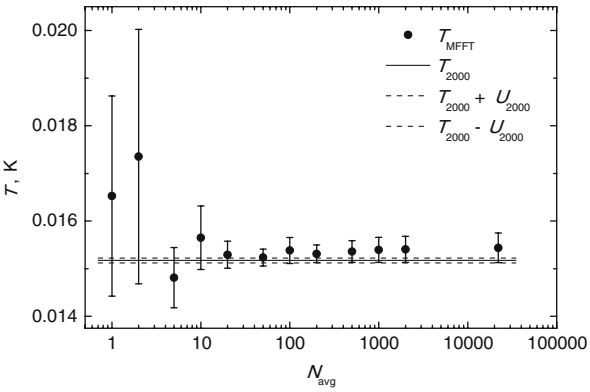

Fig. 6 T_{MFFT} versus the number of averages N_{avg} at $T_{2000} \approx 0.015\,\mathrm{K}$ for the frequency range from 10 to 400 Hz. Error bars correspond to the estimated expanded uncertainty ($k = 2$). Also indicated is the expanded uncertainty ($k = 2$) for the PLTS-2000 realization

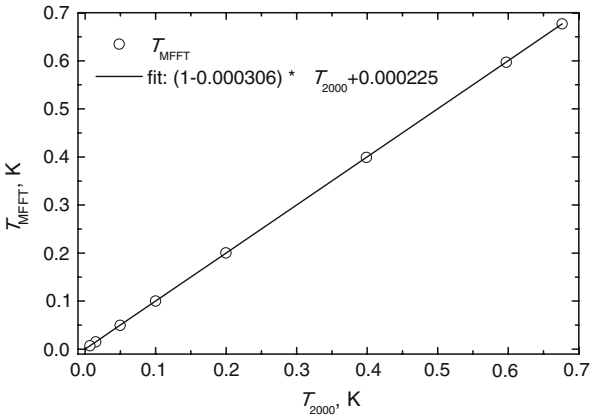

Fig. 7 T_{MFFT} in comparison with T_{2000} for the temperature range from 0.676 to 0.007 K. T_{MFFT} is calculated by averaging the TMFN spectra 22,000 times in the frequency range from 10 to 800 Hz. Linearity of T_{MFFT} in terms of T_{2000} is indicated by the fit

is well below 0.3%. However, at temperatures below 0.05 K, T_{MFFT} is systematically shifted to values higher than T_{2000} by up to 4%. In this region, the ratio of the TMFN signal to the SQUID noise is substantially reduced. In addition, an admixture of an excess low-frequency noise contribution can be assumed as it is visible from the lowest trace of the noise spectra in Fig. 3. An excess low-frequency noise component mainly results in a larger $S_0(T)$ value for the low temperature fits, causing higher T_{MFFT} values. Unfortunately, the excess noise component cannot be taken into account by the spectrum parameters deduced from the fit of the spectrum to Eq. 1 at T_{ref} where the TMFN signal is high. Low-frequency excess noise at low temperatures of unidentified origin has been observed in SQUIDs [16,17] and seems to occur in the SQUID system used here as well. Another possibility is overheating of the part of the noise sensor that is detected by the SQUID during the measurements. Nevertheless, even in the current configuration, the MFFT is highly linear in T_{2000}. A fit of the T_{MFFT} versus T_{2000} values gives a small deviation from linearity of the order of a few 10^{-4} (see Fig. 7). From the high linearity of the MFFT in terms of the realization of the PLTS-2000, we conclude that the assumption of a constant electrical conductivity is confirmed for the high-purity Cu temperature sensor used.

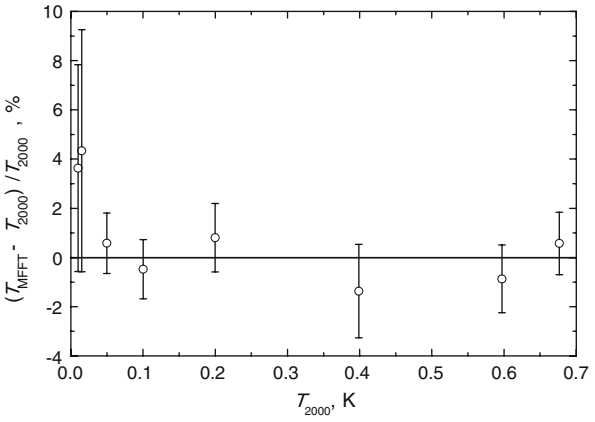

Fig. 8 Relative temperature deviation of T_{MFFT} from T_{2000} for the temperature range from 0.676 to 0.010 K. T_{MFFT} is calculated from averaging the TMFN spectra 100 times in the frequency range from 10 to 400 Hz. Error bars correspond to the estimated expanded uncertainty ($k = 2$)

The application of the MFFT as a fast secondary thermometer with a resolution of about 1% in temperature is demonstrated by the results indicated in Fig. 8. The T_{MFFT} values are calculated from the 10 to 400 Hz spectra each averaged 100 times, corresponding to $t_{\mathrm{meas}} = 200$ s (see Fig. 4). In the range from 0.6 to 0.05 K, the relative deviation from T_{2000} is below 1% except for the 0.4 K point. As in the case for the data derived from the spectra averaged over significantly longer t_{meas}, at the lowest temperatures, T_{MFFT} is also systematically shifted to higher values compared with T_{2000}. The deviations amount to about +4% at maximum.

To investigate this effect more in detail, the dependence of the noise spectra on the electrical power dissipated by the SQUID in the MFFT was inspected. A roughly linear increase of the temperature difference $T_{\mathrm{MFFT}} - T_{2000}$ is observed at 0.05 K as well as at 0.015 K for dissipation powers up to about 230 pW. If we assume that the power dissipated P is transferred directly to the electron system of the noise sensor, its overheating compared with $T_{\mathrm{ph}} = T_{2000}$ due to hot-electron effects can be estimated using the relation $T_{\mathrm{e}} = \left(P/\Sigma\Omega + T_{\mathrm{ph}}^5\right)^{1/5}$, where T_{e} is the temperature of the electron system, T_{ph} is the temperature of the phonon system, Σ is a parameter involving the electron-phonon coupling, and Ω is the volume [11]. Even when we consider for the heat exchange between the electron and phonon system only, the small volume of the thin Cu membrane of the noise sensor, the hot-electron effects contribute to the observed temperature difference not more than 10 and 0.1% at 0.015 and 0.05 K, respectively. These numbers are derived using the value $\Sigma = 1 \times 10^9\,\mathrm{W \cdot m^{-3} \cdot K^{-5}}$ for bulk Cu. In addition, a thermal decoupling of the noise sensor, i.e., large thermal gradients within the Cu parts, can be excluded for the power level under consideration.

Therefore, we attribute the observed small but systematic overheating of T_{MFFT} at temperatures below 0.05 K to additional unidentified noise sources as discussed above. To resolve this issue, another MFFT configuration with the SQUID located closer to the metallic noise sensor has been fabricated. The new MFFT setup with further reduced outer dimensions uses a SQUID gradiometer chip of 100 μm thickness only whereas the volume of the metallic noise sensor which is sensed by the SQUID remains unchanged. First tests between 1.4 and 0.2 K confirmed that the zero frequency value

$S_0(T)$ of the TMFN is approximately doubled compared to the first design. In addition, the characteristic fall-off frequency f_c was found to be nearly twice that of the older design, making the thermometer faster for a chosen uncertainty.

5 Conclusions

We have built a novel noise thermometer, a MFFT, for practical low temperature thermometry and compared it for the first time directly with a high-accuracy realization of the PLTS-2000. The integrated MFFT setup comprises a high-purity Cu noise sensor and a specially adapted SQUID gradiometer. The MFFT is simple, very compact, insensitive to external influences, and provides good thermal contact for cooling to the mK region. Over two decades, the MFFT was employed as a semi-primary thermometer in temperature from about 0.7 to 0.007 K and found to be of excellent linearity in terms of T_{2000}. For short measuring times of 200 s, the deviation of the MFFT temperature readings from T_{2000} was below 1%.

At the current stage of development, the MFFT is intended for use as a practical thermometer with a linear characteristic in a broad temperature range from 4.2 K down to below 10 mK. For this purpose, the MFFT needs to be calibrated at only a single reference temperature and uses standard SQUID technology which is commonly available in many low temperature laboratories. Further developments are directed at commercializing the MFFT in the near future and developing a MFFT design that enables its application as a primary thermometer.

References

1. H. Preston-Thomas, Metrologia **27**, 3 (1990)
2. BIPM, *Procès-Verbaux des Séances du Comité International des Poids et Mesures*, (2001), vol. 68, p. 128
3. R.L. Rusby, M. Durieux, A.L. Reesink, R.P. Hudson, G. Schuster, M. Kühne, W.E. Fogle, R.J. Soulen, D.E. Adams, J. Low Temp. Phys. **126**, 633 (2002)
4. R.L. Rusby, B. Fellmuth, J. Engert, W.E. Fogle, E.D. Adams, L. Pitre, M. Durieux, J. Low Temp. Phys. doi:10.1007/s10909-007-9502-y (in press)
5. J. Engert, B. Fellmuth, K. Jousten, Metrologia **44**, 40 (2007)
6. A. Netsch, E. Hassinger, C. Enss, A. Fleischmann, in *Low Temp. Phys.*: *24th Int. Conf. Low Temp. Phys.*, *AIP Conf. Proc.*, vol. 850, ed. by Y. Takano, S.P. Hershfield, S.O. Hill, P.J. Hirschfeld, A.M. Goldman, (AIP, New York, 2006), pp. 1593–1594
7. J. Beyer, D. Drung, A. Kirste, J. Engert, A. Netsch, A. Fleischmann, C. Enss, in *ASC 2006 Conf. Proc. IEEE Trans. Appl. Supercond.*, vol. 17 (2007), Issue 2, Part 1, p. 760
8. F. Pobell, *Matter and Methods at Low Temperatures*, 3rd edn. (Springer, Berlin, 2007), ISBN 978-3-540-46356-6 and references therein
9. T. Varpula, T. Poutanen, J. Appl. Phys. **55**, 4015 (1984)
10. B.J. Roth, J. Appl. Phys. **83**, 635 (1998)
11. F.C. Wellstood, C. Urbina, J. Clarke, Phys. Rev. **B49**, 5942 (1994)
12. J. Clarke, A.I. Braginski (eds.), *SQUID Handbook*, vol. 1 (WILEY-VCH, Weinheim, 2004), ISBN 3-527-40229-2
13. J.T. Harding, J.E. Zimmermann, Phys. Lett. **27A**, 670 (1968)
14. G. Schuster, A. Hoffmann, D. Hechtfischer, in *Realisation of the temperature scale PLTS-2000 at PTB* (PTB-Bericht, Braunschweig PTB-ThEx-21, 2001), ISBN 3-89701-742-3

15. D. Drung, M. Mück, in *SQUID Electronics* ed. by J. Clarke, A.I. Braginski. SQUID Handbook, vol. 1 (WILEY-VCH, Weinheim, 2004), pp. 127-170, ISBN 3-527-40229-2
16. F.C. Wellstood, C. Urbina, J. Clarke, Appl. Phys. Lett. **50**, 772 (1987)
17. D. Drung, C. Hinnrichs, H.-J. Barthelmess, Supercond. Sci. Technol. **19**, S235 (2006)